

## 10. INTERSTITIAL WATER STUDIES, LEG 15 – ALKALINITY, pH, Mg, Ca, Si, PO<sub>4</sub> AND NH<sub>4</sub>

Joris M. Gieskes, Scripps Institution of Oceanography, La Jolla, California

### INTRODUCTION

During Leg 15 in the Caribbean Sea, a special program for the study of the interstitial water chemistry of marine sediments was executed. The major objectives were: (1) close sampling at three sites of very different sedimentary environments to gain information on changes in the interstitial water chemistry as a function of mineralogy, depth, and possible diagenetic changes; (2) an investigation of the effect of the temperature at which the sediments are squeezed on the composition of the expressed interstitial water (c.f., *inter alia*, Mangelsdorf et al., 1969; Bischoff et al., 1970; Fanning and Pilson, 1971); (3) the sampling of gases, the collection of sediments, and other special programs.

Some shipboard measurements were carried out, such as the measurement of pH, alkalinity, and silicate contents of both warm (23°C) and cold (4°C) squeezes. Otherwise, all samples were carefully packaged and sent to various investigators for shore laboratory analyses. The results reported in this paper concern mainly the analyses carried out on board ship and additional analyses on the packaged samples that were titrated for alkalinity on the ship by the author.

Laboratory analyses were made for calcium magnesium, ammonia, and phosphate. These elements are mostly involved in the early diagenetic changes in the sediment interstitial water system, due to sulfate reduction, carbonate equilibria, and possible authigenic silicate formation.

I would like to express my sincere thanks to Dr. Wallace Broecker, and to Messrs. Ross Horowitz, Lee Waterman, Richard Dubois, and David Bos for their cheerful cooperation and all the hard work that went into making this geochemical leg a success. Special thanks go to David Bos, who was of great help in the further analyses in the author's laboratory. The punch-in electrode system was designed by Robert Berner and the flow-through electrode system was suggested by Robert Garrels.

### METHODS

This section contains brief discussions of the analytical methods used in this study. Analyses for calcium and magnesium were carried out using complexometric titrations, which yield a comparison with the analytical technique of atomic absorption spectroscopy carried out on the same samples (Sayles et al., this volume; Presley et al., this volume).

#### pH

Two different methods were used to measure the pH of the interstitial water. Measurements were carried out by inserting electrodes directly into one of the core halves

("punch-in electrodes") and by measuring the pH of the expressed interstitial water.

The punch-in electrodes consisted of an ORION® model 90-02 double junction reference electrode and a Beckman model 40471 glass electrode. The accuracy of these measurements is not better than  $\pm 0.08$  pH units.

The measurements on the interstitial water were carried out on the samples immediately after their expression into a 30 ml syringe. The water was transferred from the syringe into a specially constructed glass capillary electrode, which in turn was connected to a 25 ml glass vessel containing surface seawater. In the latter vessel, a saturated calomel reference electrode was inserted. The 30 ml syringe remained attached to the capillary electrode during the measurement so that contact with the air in the glass electrode was minimized. The electrodes were standardized with Beckman buffers pH = 6.86, 7.41, and 4.01. The calibration slope was found to be  $59.5 \pm 1.0$  mv per pH unit at  $27^\circ\text{C} \pm 2^\circ$ . The accuracy is 0.05 pH units or 3 millivolts.

During Leg 15 use was made of Whatman 40 acid washed hardened filter papers in the sediment squeezers. Usually the interstitial water would flow through two such filter papers. Subsequent investigations (Gerry Bode and Dennis Graham, personal communication) have pointed out that if  $25 \pm 5$  ml of interstitial water flows through these filters (i.e., the approximate amounts obtained during Leg 15), the alkalinity will be lowered by  $0.09 \pm 0.03$  milliequivalents/l due to "titration" by the acid residue. The data in Table 1 have been corrected accordingly – the error is small for samples with alkalinities above 5 milliequivalents/l ( $< 2\%$ ), but is 5 percent for alkalinities of about 2.0 milliequivalents/l. The data in Figures 3, 10, and 17 should be corrected by 0.1 milliequivalents/l.

#### Alkalinity

For the determination of the alkalinity, the Gran (1952) titration method was used as described by Dyrssen (1965) and by Edmond (1970). A more detailed description of the method is given by Gieskes and Rogers (in preparation).

Only the second end point of the carbonic acid system is determined so that an open vessel could be used. Titrations were carried out on 10 ml samples using 0.1517 N HCl as the titrant. A water-jacketed thermostated vessel of 15 ml capacity was used for these purposes so that measurements could be carried out at  $25.00 \pm 0.02^\circ\text{C}$ . Use was made of a Corning semimicro combination pH electrode.

The accuracy of the method is estimated to be  $\pm 0.5$  percent (Gieskes and Rogers, in preparation).

#### Calcium

Calcium was determined using the method of Tsunogai, Nishimura, and Nakaya (1968). In this method, Ethylene

TABLE 1  
pH and Alkalinity

	Squeeze Type <sup>a</sup>	Depth (m)	Flow Through		Punch In		pH	pH Saturation	Alkalinity meq/l
			t °C	pH	t °C	pH			
147-2-3/4	C	8.5	27.3	7.49			7.75		18.2
147-4-3/4	C	28	27.9	7.25			7.71		13.9
147-8-2/3	C	63	28.4	7.21			7.48		21.9
147-10-3/4	C	82	26.7	6.97	27.0	6.64	7.23		28.8
147A-1-2(96)	C	2.5	27.6	7.36			7.62	7.0	15.0
	W		27.6	(6.77)	22.0	6.93	(6.81)		—
147B-1-3(110)	C	4.25	27.8	7.28			7.54	7.15	18.2
	W		27.8	(6.20)	23.5	7.01	(6.24)		—
147B-1-4(15)	C	4.75	28.0	7.58			7.84	7.5	18.1
	W		27.7	7.62	24.0	7.36	7.66		
147B-1-4(35)	C	4.85	28.0	7.62			7.88	7.35	17.7
	W		28.0	7.57	22.0	7.16	7.61		18.2
147B-1-4(57)	C	5.1	28.0	7.56			7.82	7.45	15.6
	W		28.0	7.52	24.8	7.19	7.56		
147B-2-2(00)	C	15	28.2	7.30			7.56		8.5
	W		28.2	7.29	25.0	7.05	7.33		8.2
147B-2-6(00)	C	21	26.4	7.37			7.61	7.2	14.2
	W		26.4	7.29	25.7	6.94	7.32		14.7
147B-6-2(44)	C	51	27.9	7.55			7.81	7.4	10.4
	W		27.9	7.59	27.0	7.03	7.63		
147B-7-4(36)	C	63	28.4	7.34			7.70	6.8	25.3
	W		28.4	7.35	28.0	6.76	7.39		
147B-9-4(65)	C	83	29.4	7.05			7.33	6.7	28.5
	W		29.4	6.95	26.0	6.71	7.02		28.9
147B-11-3(28)	C	100	29.0	7.17			7.43	6.6	
	W		29.0	7.05	27.5	6.72	7.09		35.2
147C-2-1(41)	C	126	27.9	7.12			7.38	6.55	33.8
	W		27.9	6.94			6.98		
147C-4-4(34)	C	148	27.2	7.11			7.36	6.58	32.2
	W		27.2	6.98			7.02		31.6
147C-7-4(91)	C	176	27.4	7.43			7.69	6.65	24.3
	W		27.4	7.42			7.46		—
148-1-4(105)	C	6	29.0	7.53			7.80	7.65	4.2
	W		28.5	7.43	20.0	7.37	7.48		4.35
148-1-2(105)	C	3	29.5	7.64			7.90		3.0
	W		29.5	7.54	19.5	7.34	7.59		3.55
148-2-1(60)	C	11	28.0	7.46			7.72		3.7
	W		28.0	7.92	18.0	7.89	7.96		3.5
148-2-3(90)	C	13	28.6	7.61			7.88		4.6
	W		28.6	7.51	22.0	7.33	7.56		4.95
148-3-3(100)	C	22	26.8	7.48			7.74	7.6	5.4
	W		26.8	7.44	19.0	7.42	7.48		5.6
148-4-3(90)	C	31	28.1	7.45			7.71		5.2
	W		28.1	7.42	19.0	7.43	7.46		4.95
148-5-2(105)	C	39	28.5	7.46			7.72		
	W		28.5	7.42	18.0	7.42	7.46		6.5
148-6-4(105)	C	51	29.3	(7.48)			(7.75)		6.7
	W		29.3	7.44	19.0	7.37	7.49		6.3
148-7-3(105)	C	59	29.4	7.51			7.78		7.9
	W		29.4	7.49	15.5	7.43	7.54		7.8
148-8-3(15)	C	67	29.0	7.46			7.73		
	W		29.0	7.41	17.5	7.41	7.46		8.35
148-9-4(105)	C	79	28.9	7.65			7.92		8.0
	W		28.9	7.60	17.0	7.47	7.65		8.05
148-10-3(105)	C	86	28.0	7.61			7.87	7.6	6.95
	W		28.0	7.71	19.0	7.52	7.75		7.15
148-12-4(105)	C	106	27.8	(7.72)			(7.98)	7.65	5.5
	W		27.8	7.53	20.0	7.36	7.57		5.8
148-14-3(105)	C	122	28.6	7.50			7.76		5.0
	W		28.6	7.42	20.0	7.51	7.46		5.4
148-16-3(105)	C	141	28.2	7.43			7.69		3.8
	W		28.2	7.30	21.5	7.33	7.34		
148-18-2(105)	C	159	27.4	7.61			7.87	7.6	3.9
	W		27.4	7.51	22.0	7.38	7.55		4.15
148-20-3(105)	C	179	28.0	7.42			7.68		3.8
	W		28.0	7.42			7.46		3.9

TABLE 1 – Continued

Sample	Squeeze Type <sup>a</sup>	Depth (m)	Flow Through		Punch In		pH	pH Saturation	Alkalinity meq/l
			t°C	pH	t°C	pH			
148-23-4(95)	C	209	30.0	7.40			7.67	7.45	3.2
	W		30.0	(7.73)			(7.78)		3.2
148-26-2(15)	C	232	30.1	7.49			7.78	(7.5)	2.5
	W		30.1	7.42			7.48		3.1
149-2-2(105)	C	4	30.0	7.51			7.80	8.0	2.4
	W		30.0	7.47	20.0	7.44	7.55		2.6
149-2-5(105)	C	8	30.0	7.49			7.78		2.5
	W		30.0	7.46	20.0	7.40	7.54		2.7
149-3-5(105)	C	17	29.0	7.28			7.56	7.85	2.7
			29.0	7.37	20.0	7.30	7.44		2.9
149-4-3(105)	C	23	28.4	7.35			7.63		2.6
	W		28.4	7.35	20.0	7.32	7.41		2.85
149-5-3(120)	C	32	26.9	7.46			7.71		2.6
	W		26.9	7.44	20.0	7.33	7.48		2.7
149-6-4(105)	C	43	27.0	7.38			7.63		2.2
	W		27.0	7.30	20.0	7.33	7.34		2.45
149-7-2(105)	C	49	25.8	7.32			7.57	7.80	2.3
	W		25.8	7.27	20.0	7.36	7.30		2.5
149-8-4(105)	C	62	26.0	7.32			7.57		2.2
	W		26.0	7.32	20.0	7.29	7.35		2.4
149-9-5(105)	C	72	26.8	7.24			7.49		1.9
	W		26.8	7.24	20.0	7.33	7.28		2.2
149-10-2(120)	C	78	29.2	—			—	7.8	1.9
	W		29.2	—	20.0	7.38	—		2.05
149-11-4(120)	C	90	29.0	7.23			7.52		1.8
	W		29.0	7.23	20.0	7.38	7.31		1.9
149-12-5(120)	C	100	29.0	7.12			7.41		1.4
	W		29.0	7.21	20.0	7.40	7.29		
149-14-3(120)	C	116	29.0	7.21			7.49	7.6	1.9
	W		29.0	7.14	20.0	7.40	7.22		2.05
149-16-4(15)	C	135	29.0	(7.06)			(7.34)	7.7	1.9
	W		29.0	6.95	20.0	7.01	7.03		2.45
149-18-3(120)	C	153	29.0	7.13			7.41		2.3
	W		29.0	7.12			7.20		2.4
149-20-4(120)	C	173	29.0	7.03			7.31	7.3	3.2
	W		29.0	7.03	20.0	7.05	7.08		3.15
149-23-4(120)	C	201	29.2	6.88			7.16	7.25	3.35
	W		29.2	6.91			6.98		3.6
149-26-2(120)	C	226	28.5	6.98			7.26		3.05
	W		28.5	6.92			6.97		3.1
149-29-3(15)	C	258	28.4	6.98			7.26		3.1
	W		28.4	6.94			6.99		2.9
149-31-1(120)	C	271	28.0	6.97			7.25		3.45
	W		28.0	7.00			7.05		3.45
149-33-1(120)	C	289	28.0	6.98			7.26	7.1	3.15
	W		28.0	6.94			7.00		3.0
149-35-4(120)	C	313	28.0	6.96			7.24		2.7
	W		28.0	6.98			7.03		2.55
149-37-3(120)	C	329	29.0	6.98			7.26		2.6
	W		29.0	7.01			7.09		2.6
149-40-1(100)	C	354	29.0	7.01			7.29	7.15	2.55
	W		29.0	7.01			7.09		2.5
149-41-5(120)	C	369	29.2	7.00			7.28		2.4
	W		29.2	7.05			7.12		2.35
149-42-2(120)	C	374	28.0	7.00			7.28		2.6
	W		28.0	7.07			7.13		2.4

<sup>a</sup>Squeeze types: C – cold, W – warm.

bis (oxyethelenenitrilo) tetra acetic acid (EGTA) is used as a titrant and 2,2'-Ethane-diylidene dinitrilo-diphenol (GHA) is used as the indicator. The calcium-GHA complex is extracted quantitatively into a layer of *n*-butanol.

Using an Eppendorf pipette 1.00 ml of sample and 1.00 ml of 5 or 10 mM EGTA were added into a 15 ml titration vessel. While stirring the solution with a Teflon-

covered magnetic stirring bar, 0.5 ml of 0.04 percent GHA and 0.5 ml of buffer solution was added. After stirring for about 3 minutes 1 ml *n*-butanol was added. Titration was accomplished with a 5 mM or 10 mM EGTA solution using a microburette with immersed tip, while stirring vigorously. Near the endpoint, stirring was stopped frequently in order to observe the color of the butanol layer. The endpoint is

characterized by a change from red to colorless.

Tsunogai et al. (1968) report that, for seawater, a correction factor of 0.9946 for the titer of the EGTA solution is needed in order to correct for magnesium and strontium. The error caused by magnesium is small, 0.26 percent, at seawater values and rapidly vanishes with decreasing magnesium concentrations. About 90 percent of the strontium is determined and, hence, corrections are made for this. At seawater concentrations, this correction is about 1 percent of the sum of Ca and Sr. In this report, these corrections have been made using the data from Manheim et al. (this volume). In general, the accuracy of this method is about 1 percent, with a reproducibility of 0.4 percent.

#### Total Calcium, Magnesium, and Strontium

For the determination of the alkaline earth elements Ca, Mg, and Sr, the complexometric titration with EDTA was used. Again *n*-butanol was used as an extractant and this was found to be an improvement over the original method for the determination of the endpoint. The reagents used are as follows:

**EDTA:** 11.17 grams of EDTA (sodium salt) dissolved in 1 liter of distilled water to yield an approximately 0.03 M solution. Standardization was accomplished with Ultrex  $\text{CaCO}_3$  with a known Mg-background.

**Solids:** Potassium cyanide (KCN) and hydroxylamine-hydrochloride.

**Buffer:** 67.5 grams of  $\text{NH}_4\text{Cl}$  and 570 ml  $\text{NH}_4\text{OH}$  dissolved in water and the final volume made up to one liter.

**Indicator:** 0.1 gram of Eriochrome Black-T dissolved in 100 ml of 80 percent ethanol solution.

The procedure used is as follows: To a 1.00 ml sample, of interstitial water, 1 to 1.5 ml distilled water were added as were a few crystals of KCN and hydroxylamine-hydrochloride (as trace metal complexing agents). While 1 ml of ammonia buffer and 0.1 ml of indicator solution were added. While stirring 2 ml of *n*-butanol were added. Titration was done with a microburette with its tip immersed below the organic layer. Color change is red to blue. The accuracy is about 1 per cent with a reproducibility of 0.5 per cent.

#### Ammonia

Ammonia was determined by the method of Solorzano (1969) as modified by Presley (1971) to suit interstitial water analysis. Lesser amounts of catalyst were used, thus reducing the blank value appreciably; however, frequent appropriate dilutions have to be made. The accuracy is estimated to be about 5 per cent.

#### Dissolved Inorganic Phosphate

This method is essentially the same as the one described by Presley (1971) as a modification of the method of Strickland and Parsons (1968). We carried out the measurements on undiluted samples. Concentrations should be below about 21 micro-gram-atoms  $\text{PO}_4(\text{P})/\text{liter}$  or 2 ppm, because higher concentrations do not have linear absorbance characteristics. The accuracy is about 5 percent, with a lower detection limit of 0.3 micro-gram-atoms  $\text{PO}_4(\text{P})/\text{liter}$ .

#### Dissolved Reactive Silicate

Dissolved reactive silicate was measured on board ship using a modification of the method of Strickland and Parsons (1968). The data are presented in the report of Sayles et al. (this volume). Graphical representations of the data in micro-gram-atoms per liter are given in Figures 4, 11, and 18.

#### SITE DESCRIPTIONS

The sites chosen for this geochemical leg represent varied sedimentary environments.

Hole 147, drilled at a water depth of 883 meters, is in the Cariaco Trench, an anoxic basin (Richards and Vacarro, 1956) off the coast of Venezuela. The sedimentation rate is high at about 0.05 cm/y. Heezen et al. (1958) reported a sharp lithological change at a depth of about 5 meters in the sediment. Two layers of gray and brown can be distinguished in the otherwise greenish gray sediment. The age of the upper transition is estimated at 11,000 years. The presence of benthic foraminifera and the absence of fishbones as reported by Heezen et al. (1958) suggest aerobic conditions during the deposition of the gray and brown horizons. From the preliminary description of Hole 147 by Edgar et al. (1971), it appears that such gray and brown layers are again observable at 101-103 meters and 116-119 meters. The mineralogy of the gray and brown layers at 5 meters indicates a very high mica (40%) and quartz content (31-33%). The calcium carbonate is low at 3.5 percent (Schneidermann, personal communication). From this and from the studies of Heezen et al. (1958), it appears that these layers, at least those at 5 meters, may represent an ice age transition and are of terrigenous origin (turbidity currents?). Interestingly, Donnelly (this volume) reports the occurrence of gypsum at depths of 5-8, 15-17, 101, 103, and 106-115 meters. It appears that during the low seawater level conditions that are commonly associated with ice ages, the Cariaco Trench may have shown the characteristics of an evaporite basin. Donnelly (this volume) also reports the appearance of dolomite at 15-17 meters, and finds this mineral persistent below 33 meters.

Hole 148 drilled at a water depth of 1223 meters, is situated at the edge of the Aves Ridge. This hole consists mainly of grayish green calcareous clays and marls containing ash beds (Edgar et al., 1971). A more detailed description is published elsewhere in this volume. Siderite has been reported at depths from 106 to 108 meters, and at various levels deeper in the hole. The rate of sedimentation is estimated to be about 5.5 cm/10<sup>3</sup>y.

Hole 149 in the Venezuela Basin was drilled at a water depth of 3972 meters. The lithological sequence is characterized by a transition at a depth of about 200 meters from foraminiferal clay oozes and chalks to radiolarian oozes with high calcium carbonate content.

In Figure 1, the main features of the sedimentological sequences of Holes 147, 148, and 149 are represented graphically. The same depth scale is used as in all subsequent figures, so that direct comparisons can be made.

#### RESULTS

The data for pH and alkalinity are reported in Table 1. The temperatures recorded in the third and fifth columns



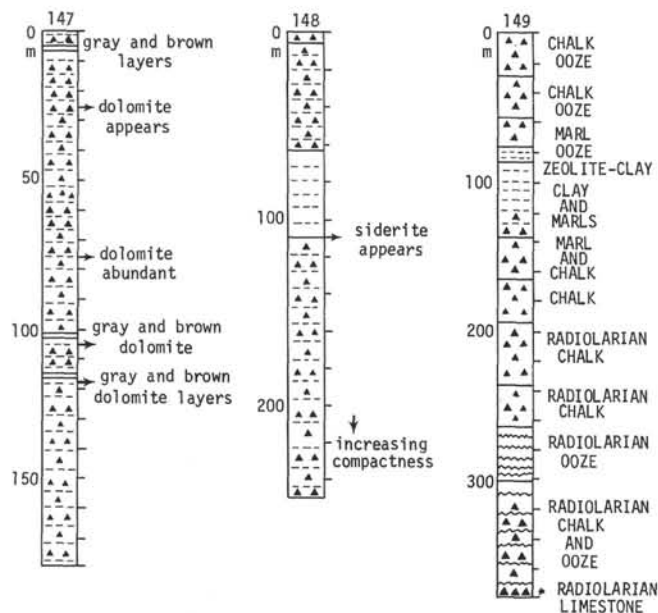


Figure 1. *Lithology.*

are the temperatures at which the pH readings were made. The seventh column gives the pH values for the squeezed water corrected to 23°C (warm squeeze) or to 4°C (cold squeeze). A temperature coefficient of 0.01 pH unit/°C was used.

In general, the samples were stored for periods of 10 to 20 hours at 4°C in a cold box. Then they were transferred into the precooled cold squeezer and then into the warm squeezer. The cold squeezer usually warmed up slightly during handling (to 8 or 10°C) and squeezing was only started after the temperature was again steady at 4°C. The temperature of the warm squeeze was not measured, but squeezing started soon after the filling of the squeezer with cold sediment. The duration of squeezing extended from a few minutes (radiolarian oozes) to nearly an hour (clays). It is therefore possible that in the former, room temperature was not reached, whereas in the latter it was. In general, the warm squeeze is estimated to have had a temperature of  $23 \pm 2^\circ\text{C}$ . Of course, the temperature effects reported here are approximate because of the lack of exact temperature control.

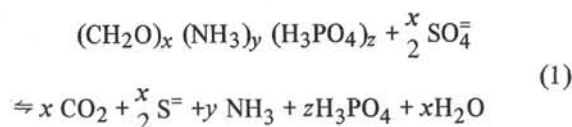
## DISCUSSION

In the following, a brief and qualitative discussion is given of the various features observed in this study.

### Alkalinity and Related Changes

In this study, particular emphasis was given to obtaining very accurate data on the alkalinity of the interstitial water. The alkalinity of the interstitial water, although it constitutes a final result of many possible reactions, does represent a useful indicator of diagenetic processes especially in sediments with relatively large rates of accumulation, one often observes relatively large depletions in dissolved sulfate in the interstitial waters. Such a sulfate depletion is generally accompanied by changes in the

following interstitial water constituents: calcium (depletion), magnesium (depletion), potassium (depletion or increase), alkalinity (increase), ammonia (increase), and inorganic phosphate (increase). Similar to Richards (1965), one can write



In oceanic organic matter one uses the average composition of oceanic plankton to obtain the coefficients  $x$ ,  $y$  and  $z$ , i.e., C:N:P=106:16:1. In marine sediments, the C:N:P ratio of organic matter is more variable (Bader, 1955), so that in order to predict the amount of ammonia and orthophosphate formed upon sulfate reduction, one should have information on the average value of the C:N:P ratio in the sedimentary organic matter. Sholkovitz (1972) was very successful in predicting ammonia and phosphate from a knowledge of this ratio in the sediments of the Santa Barbara Basin.

Subsequent to reaction (1) most of the sulfide is removed as pyrite whereas the liberated  $\text{CO}_2$ ,  $\text{NH}_3$ , and  $\text{H}_3\text{PO}_4$  appear predominantly as the species  $\text{HCO}_3^-$ ,  $\text{NH}_4^+$  and  $\text{HPO}_4^{2-}$  in the pH range of pore waters, i.e., pH=7 to 8. A sharp increase in the carbonate alkalinity can result in supersaturation with respect to calcium carbonate with a subsequent precipitation of this compound.

Various mechanisms and models have been proposed that attempt to explain the above mentioned changes (e.g., Berner et al., 1970; Drever, 1971). The latter author concerned himself particularly with the relationship between sulfate reduction and magnesium depletion. In order to test such models, it is of prime importance to obtain mass balances with a high degree of precision. In this way, Sholkovitz (1972) was able to demonstrate that sulfate reduction was quantitatively related to changes in alkalinity, calcium, ammonia, and phosphate, making it necessary to explain depletions in magnesium by processes not involving a change in alkalinity.

In the first few meters of sediments from Hole 147, and in the first 70 meters in Hole 148, an approximate mass balance can be written for changes in sulfate, ammonia, alkalinity, calcium, and magnesium, suggesting that changes in magnesium are related to changes in alkalinity in whatever process is responsible for this magnesium depletion.

In the first few meters of Hole 147, one has a seemingly linear decrease in sulfate, calcium, and magnesium, and a linear increase in ammonia, phosphate, and alkalinity (Figures 2-8). At a depth of 5 meters we observe (values approximate):  $\Delta\text{SO}_4 = -28$  mmoles/liter,  $\Delta\text{Ca} = -9$  m-gram-atoms/liter,  $\Delta\text{NH}_4 = 2.5$  mmoles/liter,  $\Delta\text{PO}_4 = 0.055$  mmoles/liter, and  $\Delta\text{alkalinity} = 16$  mequivalents/liter. If magnesium would be of importance in this mass balance we would expect a change in magnesium of  $-9$  m-gram-atoms/liter, which is close to the observed change. In addition, the linear changes in ammonia and phosphate suggest an organic matter composition of C:N:P = 100:4.5:0.1. Sholkovitz (1972) used a ratio of 106:8:0.5 in

the rapidly accumulating sediments in the Santa Barbara Basin. Longer exposure of dead planktonic organic matter at the surface of the sediment in the anaerobic waters of the Cariaco Trench has most likely caused a relatively larger removal of nitrogen- and phosphorus-containing components of the organic matter.

Below 5 meters in the Hole 147 sediments, one observes reversals in the alkalinity, calcium, and phosphate concentrations. Even though a similar mass balance as presented in the previous paragraph can be written, it seems clear that secondary processes have taken over, or that a shift in the importance has occurred in the processes that contribute to the mass balance in the upper 5 meters. In the absence of information on the solid phases that are related to these processes, it seems only of academic value to speculate on the exact significance of these changes. The disappearance of phosphate, below 5 meters for instance, could be due to calcium phosphate formation; the amounts involved, however, would be so small that they would not be detectable.

Below 60 meters in Hole 147, a sharp increase occurs in ammonia and in alkalinity, which is clearly due to the process of fermentation as suggested by the high  $\text{CH}_4$  and  $\text{CO}_2$  contents in the gas pockets of these sediments. No large changes occur in calcium and magnesium.

In Hole 148, we also observe large changes in sulfate (see Sayles et al., and Presley et al., this volume), in alkalinity, ammonia, calcium, and magnesium (Figures 9 to 15). The gradients are less pronounced due, in part, to the much lower rate of sedimentation in this area. One important observation is the 1:1 relationship between the change in the alkalinity (mainly bicarbonate) and the total carbon dioxide. More than just carbonate equilibria must be involved to explain these changes. Of course, silica reconstitution often involves changes in the  $\text{CO}_2$  equilibria, c.f., the pH. Below 100 meters, siderite is reported to occur, so that this mineral is indeed one of the likely products of the diagenetic changes as recorded in the interstitial waters.

In Hole 149 (Figures 16-22), which has a relatively low rate of accumulation, the alkalinity does not reflect the sulfate reduction process as discussed above. The alkalinity (Figure 17) changes only very little, and seems strongly correlated with the type of sediment, c.f., Figure 1. In the zeolitic clay layers, alkalinity values are substantially lower than that of seawater. Changes in calcium and magnesium seem not directly related to the sulfate reduction process. The latter process is reflected in the small, but significant increase in dissolved ammonia (Figure 19).

One interesting observation is the decrease in ammonia towards the bottoms of Holes 148 and 149. It is not clear what the exact cause of this phenomenon is; however, it does seem to be real.

### pH Measurements

The pH data tabulated in Table 1 show that the pH values of both the warm and the cold squeezes are generally very similar when measured at the same temperature. This, of course, is also a reflection of the fact that no large changes are observed in alkalinity.

A more disturbing aspect is the deviation between the punch-in electrode measurements and the warm squeeze pH values. These pH data should be in agreement to within 0.1

pH unit. In Hole 147, the disagreement is about  $0.4 \pm 0.1$  pH unit, in Hole 148 about 0.1 pH unit, and in Hole 149 there is essential agreement. In many of the squeezes in Hole 147 the extruded water was observed to effervesce, and the accompanying  $\text{CO}_2$  loss could explain the high pH values obtained from the warm squeeze. Also, the possibility exists that the warm squeeze was not truly in equilibrium, so that the measured pH would be invalid.

Most of the foraminifera and nannoplankton consist of almost pure calcite. Therefore, it was assumed that the interstitial water was in equilibrium with calcite. From the data on calcium and alkalinity (assuming the alkalinity to equal the carbonate alkalinity), and an estimate of the in situ pressure (hydrostatic) and temperature (temperature gradient  $5^\circ\text{C}/100\text{ m}$ ), the in situ pH can be estimated using the necessary constants presented by Edmond and Gieskes (1970). The calculated values are given in Table 1, and are also represented in Figures 2, 9, and 16.

Of course, the constants presented by Edmond and Gieskes (1970), are only strictly valid for seawater. In interstitial waters which show significant changes in the composition with respect to the major constituents these constants are not strictly valid, and could be modified using chemical models such as those of Garrels and Thompson (1962). To demonstrate that such calculations are possible, we particularly used Hole 149, in which changes in calcium and magnesium are equal but opposite in sign, thus virtually not affecting the values of the apparent dissociation constants.

From Figure 2, one deduces a minimum pH value of 6.6 in the lower part of Hole 147, a value which would not be incompatible with the high  $\text{CO}_2$  partial pressures observed in the gas pockets that formed in the cores (Hammond et al., this volume). The calculated pH value in the upper part is higher than the punch-in pH value, but then, of course, the punch-in pH measurements were made at  $24^\circ\text{C}$ , whereas the in situ temperature was about  $18^\circ\text{C}$  in the surface layers of the sediment.

The calculated pH values for Hole 148 are in reasonable agreement with the measured data (Figure 9). Note that the surface sediment has a temperature of about  $5^\circ\text{C}$ , and also that the warm and cold squeeze pH values have not been corrected for pressure effects.

Hole 149 presents an interesting problem. Calculations of the pH at in situ pressure and temperature yields data that appear too high. The results of the calculations are given in Table 3, where the "observed" pH value is corrected to in situ conditions. If, however, we assume that, upon storage for 10 to 20 hours at  $4^\circ\text{C}$  and 1 atmosphere, the calcium carbonate is reequilibrated, then we should calculate the equilibrium pH on this basis. The results as given in Table 3 indicate good agreement. Of course, if the sediment has reequilibrated at  $4^\circ\text{C}$  and 1 atm, then the question remains of whether the calcium and alkalinity would change as a function of pressure, or whether the effects of temperature and pressure on the pH are balanced by the change in the solubility of the calcium carbonate, thus resulting in little change in calcium and alkalinity. In general, however, the pH as calculated from the calcite equilibrium assumption is probably as good as the pH obtained from actual measurements, if not better.

Dots indicate warm (23°C) squeezes; crosses indicate cold (4°C) squeezes; triangles indicate punch in pH readings; circled dots indicate pH values calculated for Calcium carbonate saturation.

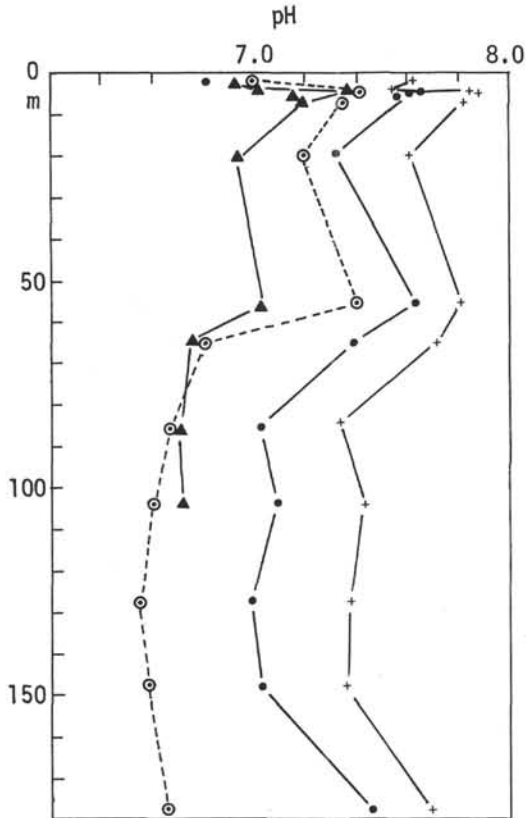


Figure 2. Site 147 - pH.

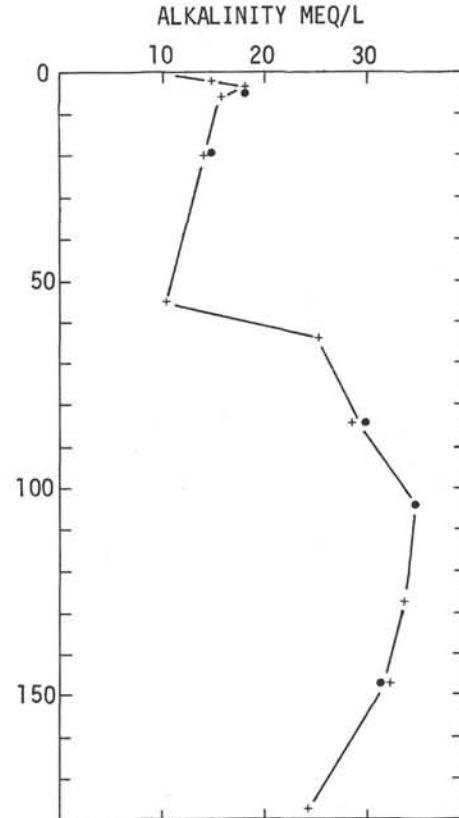


Figure 3. Site 147 - alkalinity.

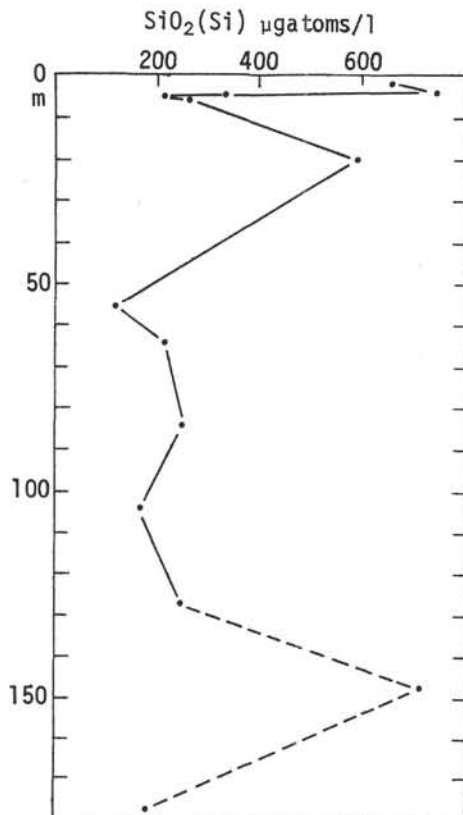


Figure 4. Site 147 - silicate.

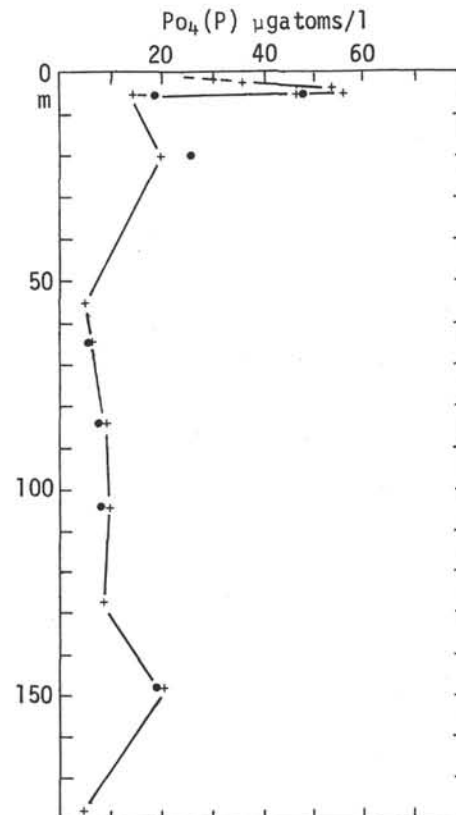


Figure 5. Site 147 - phosphate.

Dots indicate warm (23°C) squeezes; crosses indicate cold (4°C) squeezes; triangles indicate punch in pH readings; circled dots indicate pH values calculated for Calcium carbonate saturation.

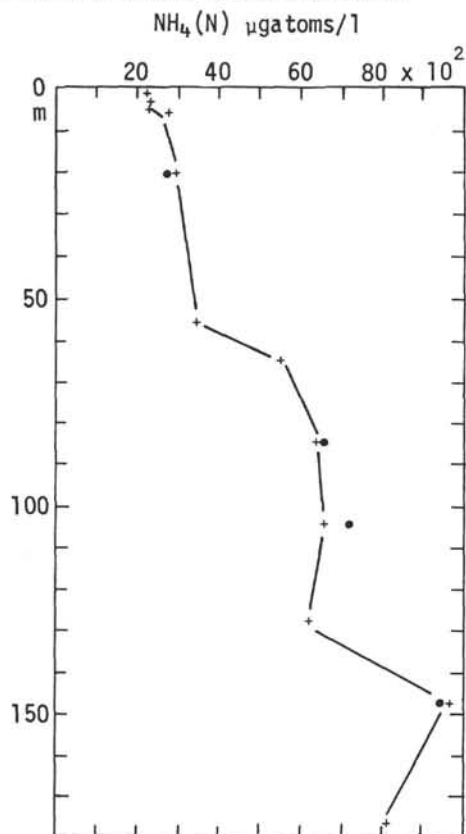


Figure 6. Site 147 - ammonia.

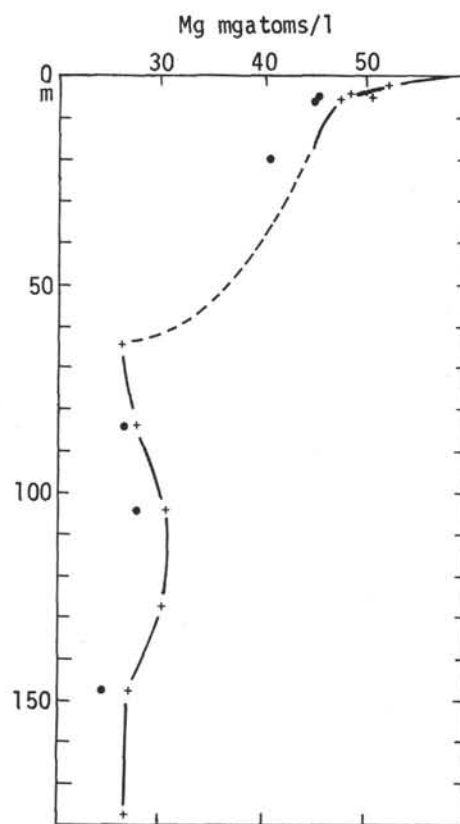


Figure 7. Site 147 - magnesium.

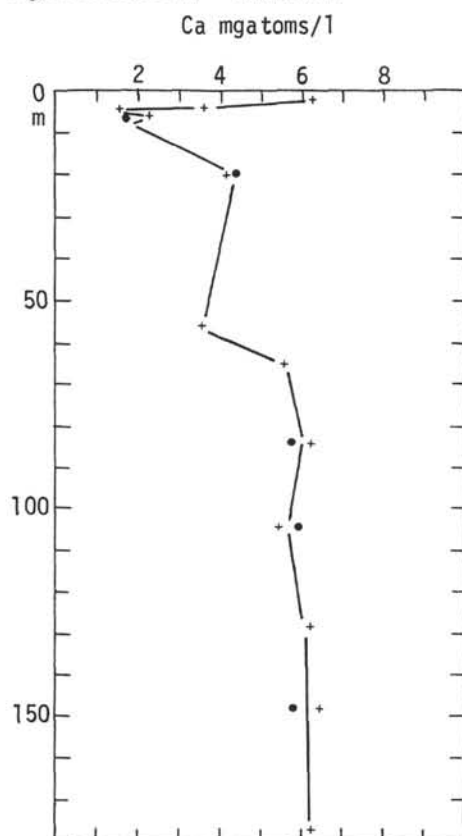


Figure 8. Site 147 - calcium.

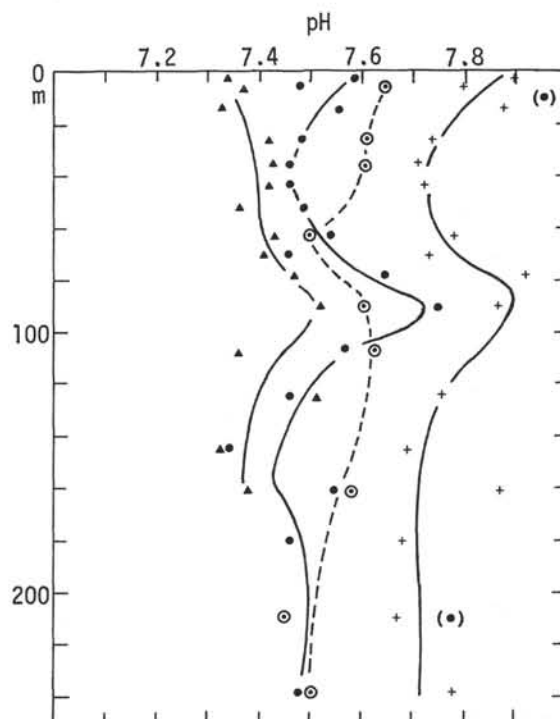


Figure 9. Site 148 - pH.



Dots indicate warm (23°C) squeezes; crosses indicate cold (4°C) squeezes; triangles indicate punch in pH readings; circled dots indicate pH values calculated for Calcium carbonate saturation.

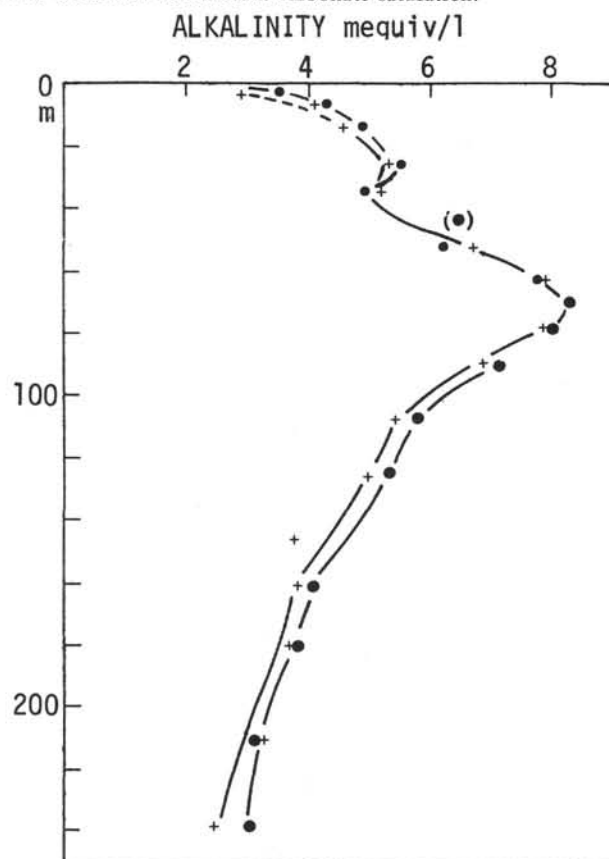


Figure 10. Site 148 - alkalinity.

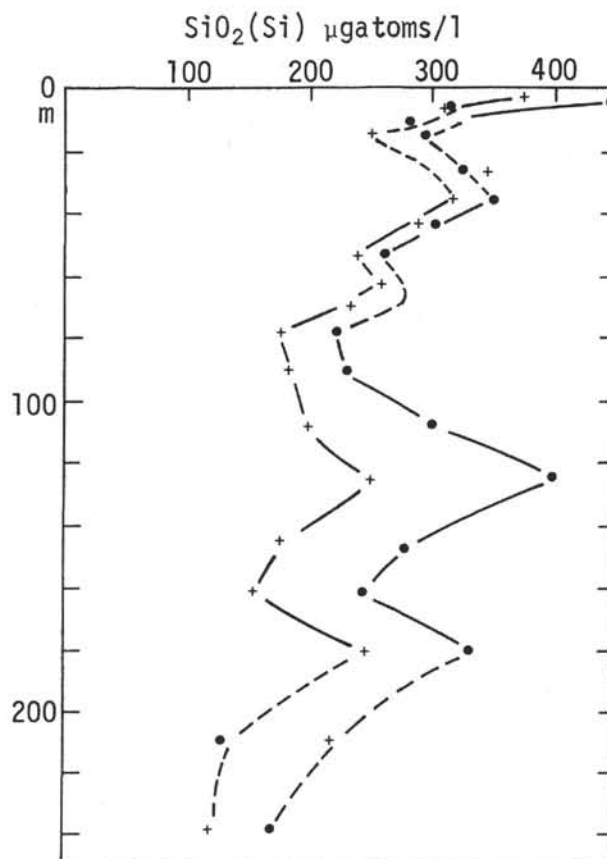


Figure 11. Site 148 - silicate.

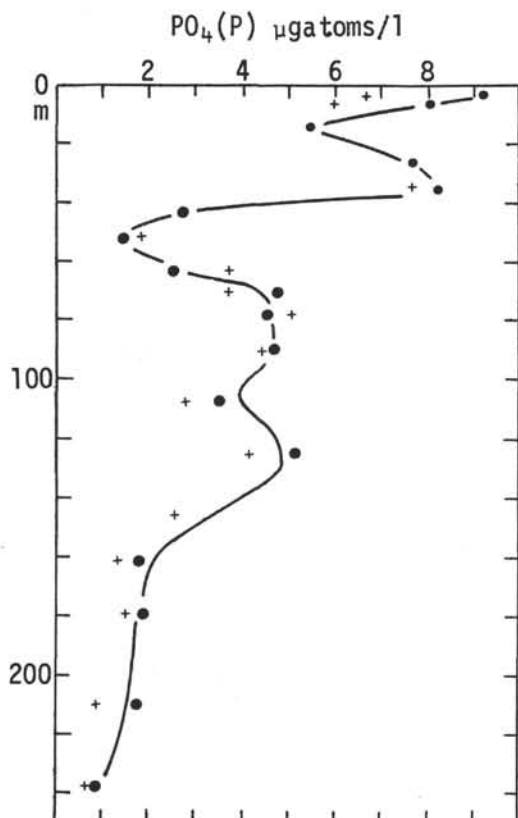


Figure 12. Site 148 - phosphate.

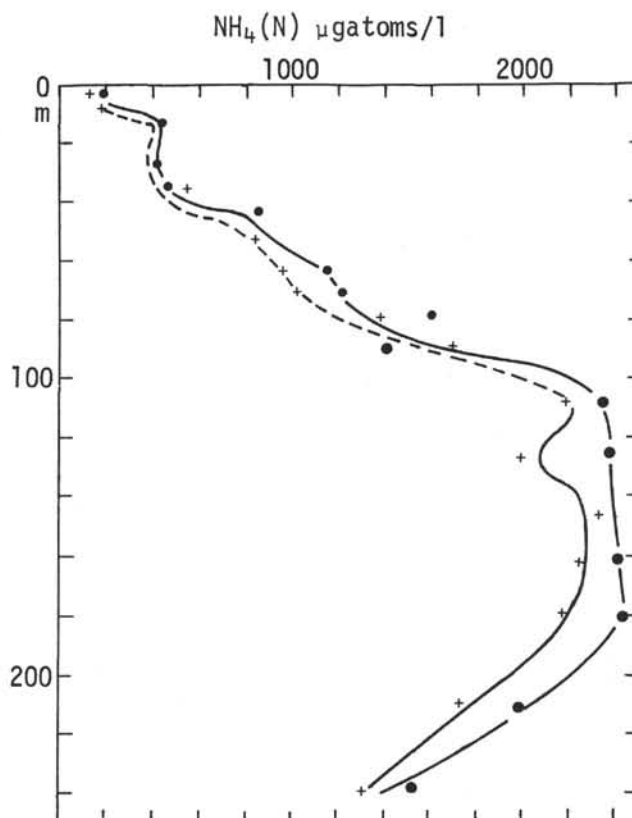


Figure 13. Site 148 - ammonia.

Dots indicate warm ( $23^{\circ}\text{C}$ ) squeezes; crosses indicate cold ( $4^{\circ}\text{C}$ ) squeezes; triangles indicate punch in pH readings; circled dots indicate pH values calculated for Calcium carbonate saturation.

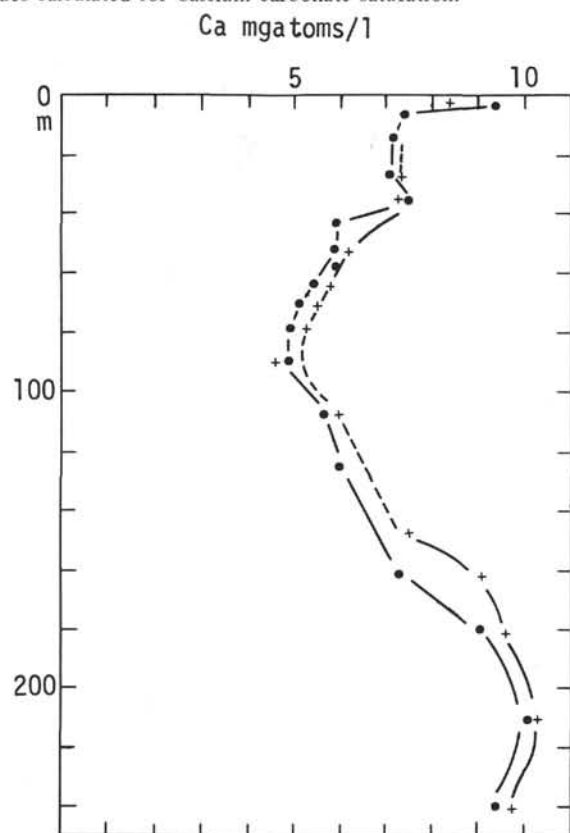


Figure 14. Site 148 - calcium.

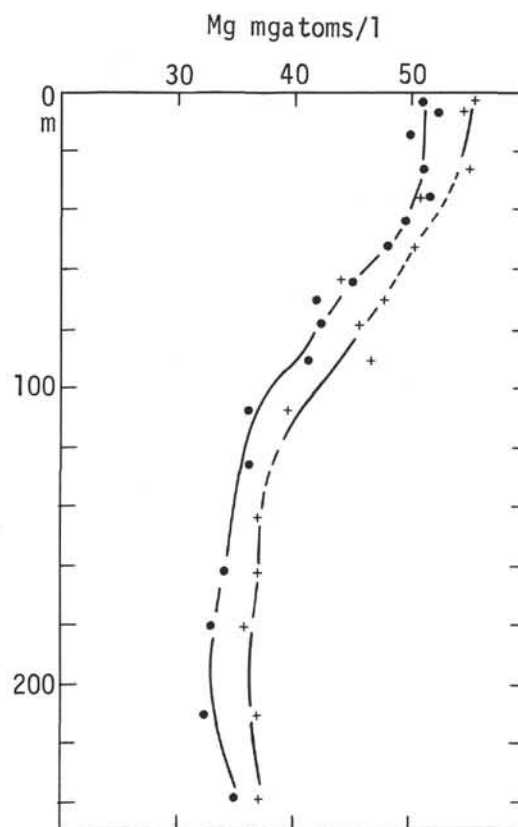


Figure 15. Site 148 - magnesium.

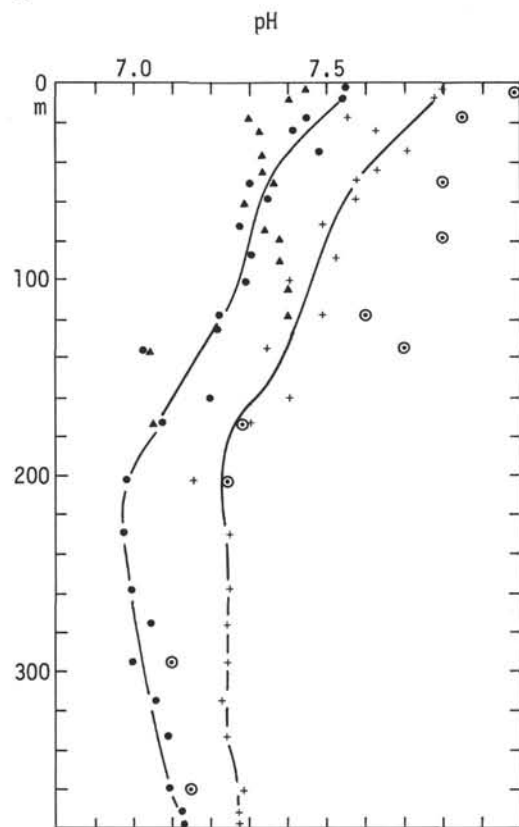


Figure 16. Site 149 - pH.

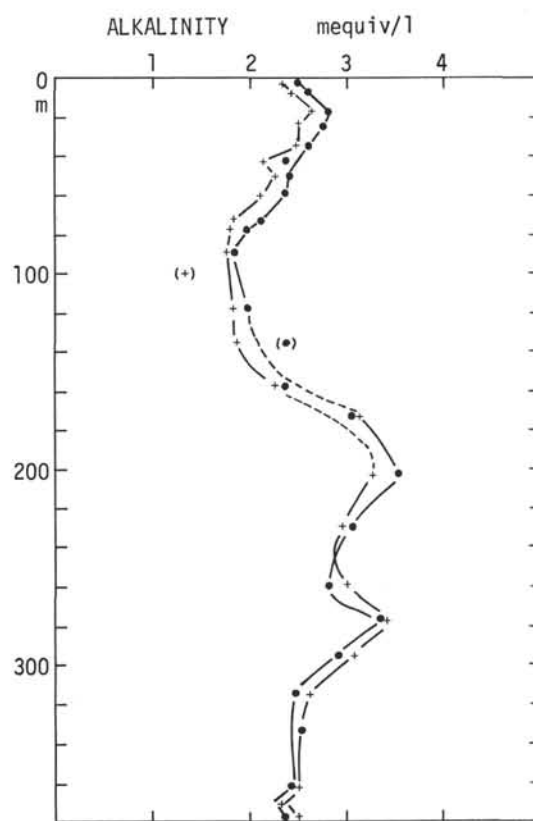


Figure 17. Site 149 - alkalinity.

Dots indicate warm (23°C) squeezes; crosses indicate cold (4°C) squeezes; triangles indicate punch in pH readings; circled dots indicate pH values calculated for Calcium carbonate saturation.

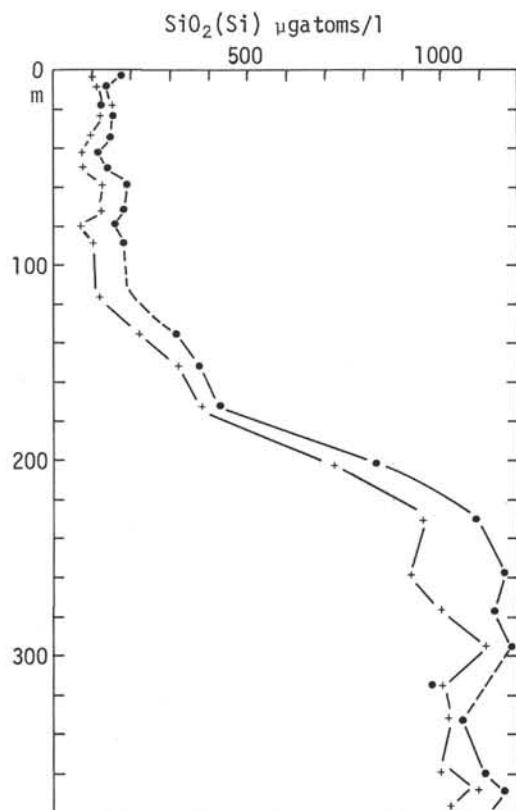


Figure 18. Site 149 – silicate.

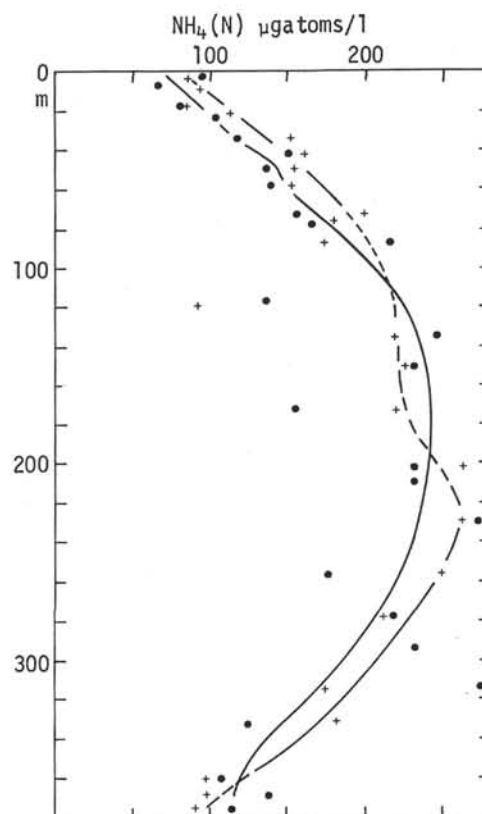


Figure 19. Site 149 – ammonia.

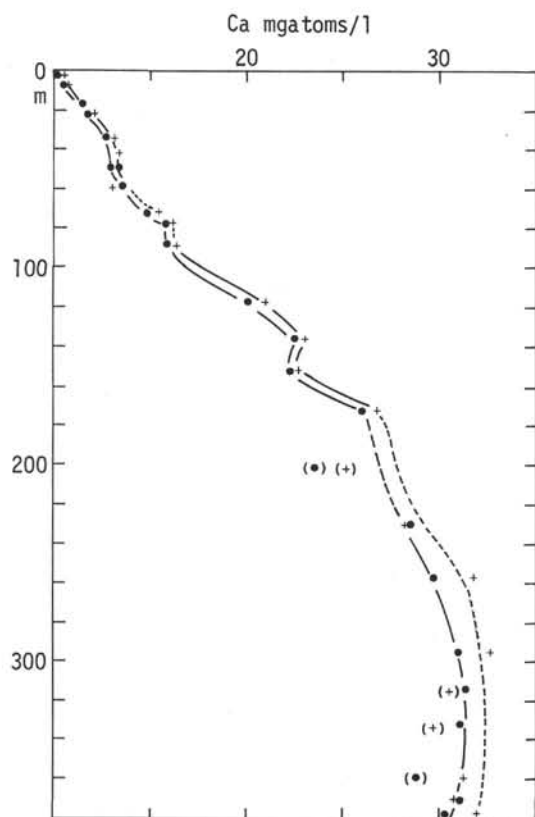


Figure 20. Site 149 – calcium.

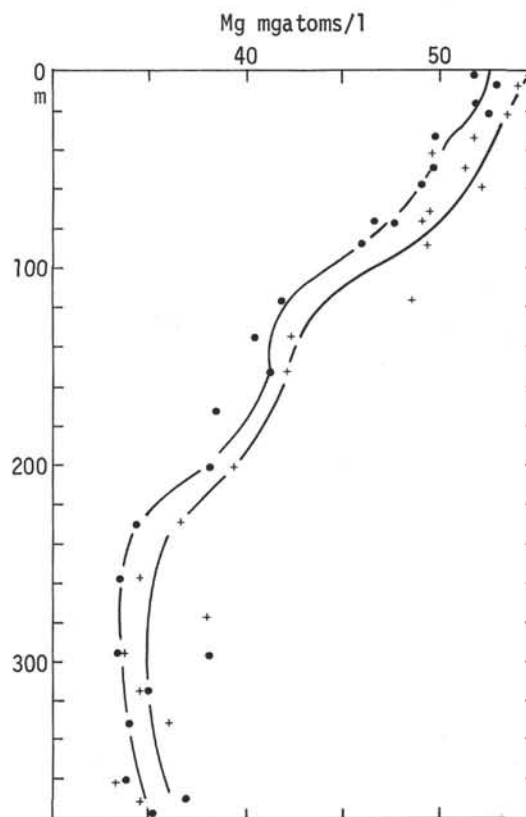


Figure 21. Site 149 – magnesium.

Dots indicate warm (23°C) squeezes; crosses indicate cold (4°C) squeezes; triangles indicate punch in pH readings; circled dots indicate pH values calculated for Calcium carbonate saturation.

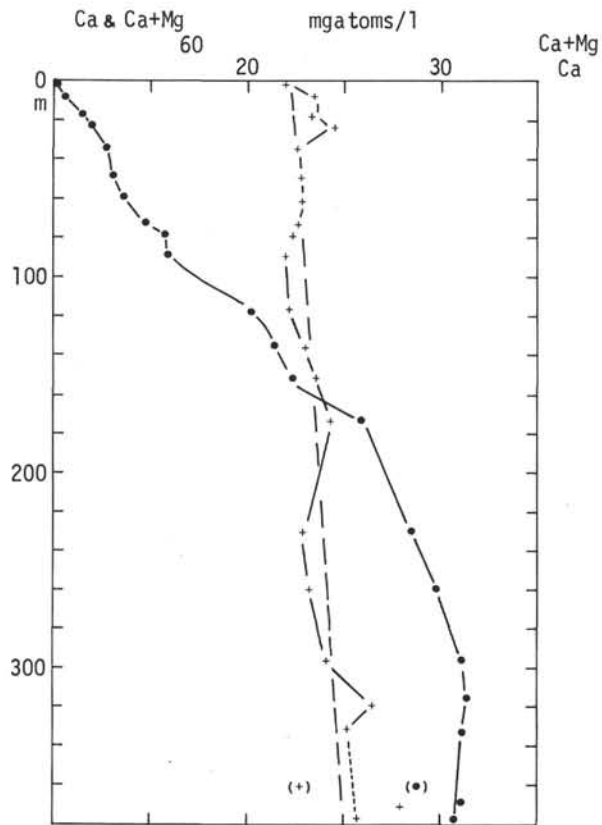


Figure 22. Site 149 – calcium and calcium + magnesium.

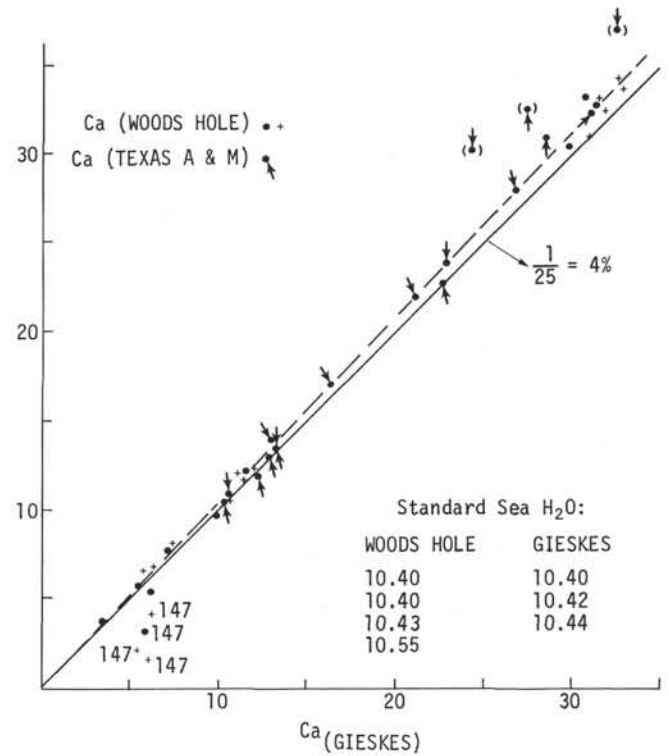


Figure 23. Calcium: atomic absorption vs. titration.

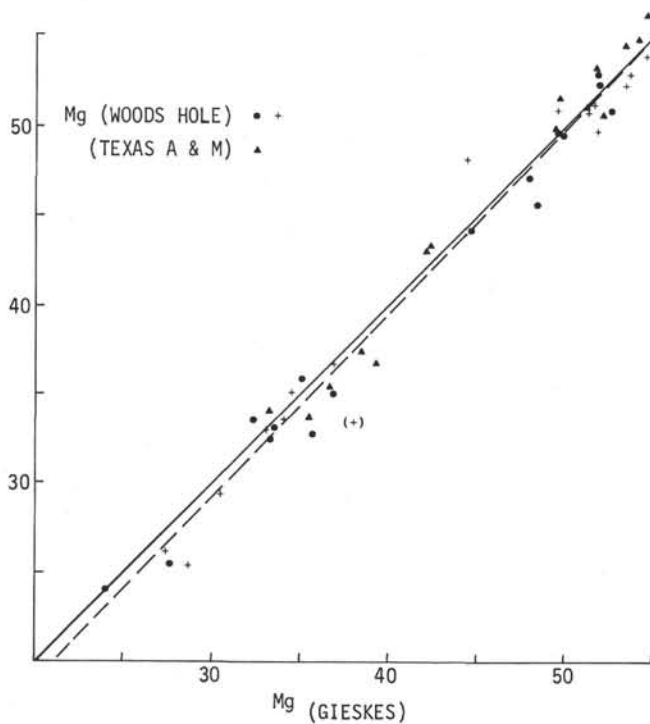


Figure 24. Mg: atomic absorption vs. titration.

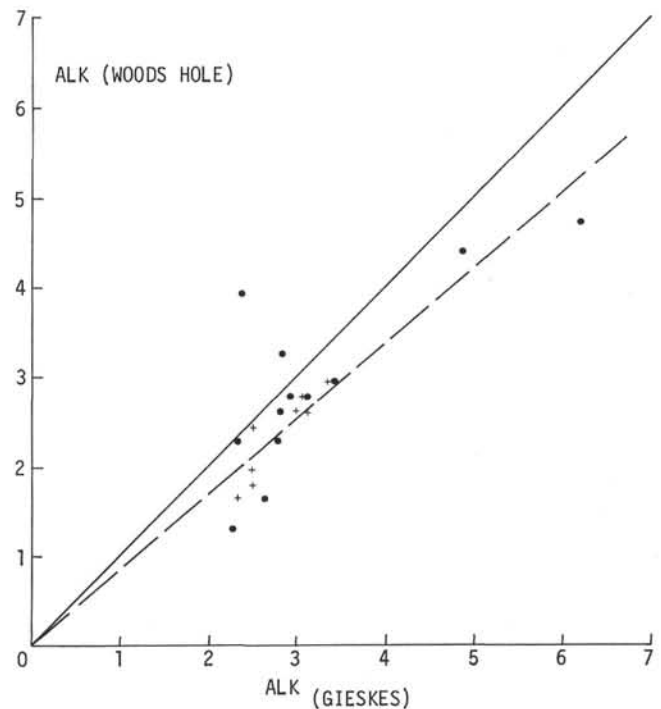


Figure 25. Alkalinity intercomparison.

TABLE 2  
Analyses for Ca, Mg, NH<sub>4</sub> and PO<sub>4</sub>

Sample	Squeeze Type <sup>a</sup>	Depth (m)	Ca (m-g-at/l)	Mg (m-g-at/l)	NH <sub>4</sub> (μ-gr-at/l)	PO <sub>4</sub> (μ-gr-at/l)
147-2-3/4	C	8.5	3.2	44.5	—	60.7
147-4-3/4	C	28	5.1	48.9	2510	15.7
147-8-2/3	C	63	5.1	31.7	5250	15.6
147-10-3/4	C	82	7.2	20.2	6800	15.4
147A-1-2(96)	C	2.5	6.1	52.1	2200	35.5
147B-1-3(100)	C	4.25	3.6	48.5	2260	53.2
147B-1-4(15)	C	4.75	1.5	50.5	2240	55.5
147B-1-4(35)	C	4.85	2.2	47.5	2250	46.0
	C		2.3	47.4	2180	47.4
	W		2.0	44.0	2240	47.3
147B-1-4(57)	C	5.1	—	—	2740	14.2
	W		1.75	45.5	2740	18.1
147B-2-2(00)	C	15	9.1	56.9	1590	27.3
	W		9.5	56.1	1600	25.3
147B-2-6(00)	C	21	4.2	44.1	2960	19.6
	W		4.3	40.6	2500	25.9
147B-6-2(44)	C	51	3.5	—	3400	5.7
147B-7-4(36)	C	63	5.5	26.2	5490	6.1
147B-9-4(65)	C	83	6.15	27.6	6370	8.6
	W		5.75	26.7	6450	7.8
147B-11-3(28)	C	100	5.45	30.6	6650	9.6
	W		6.0	27.8	7200	8.0
147C-2-1(41)	C	128	6.15	30.0	6200	8.5
147C-4-4(34)	C	148	6.4	27.0	9680	19.5
	W		5.95	24.7	9600	19.4
147C-7-4(91)	C	176	6.3	26.3	8080	4.6
148-1-2(105)	C	3	8.46	55.4	184	6.7
	W		9.41	50.9	103	9.2
148-1-4(105)	C	6	9.22	54.7	200	6.0
	W		7.38	52.2	170	8.1
148-2-1(60)	C	11	7.38	53.8	531	4.6
	W		7.11	49.7	—	3.9
148-2-3(90)	C	13	6.97	(46.7)	—	nil
	W		7.10	49.9	432	5.4
148-3-3(100)	C	22	7.37	55.0	—	—
	W		7.14	51.1	412	7.7
148-4-3(90)	C	31	7.58	50.8	550	7.7
	W		7.60	51.6	450	8.2
148-5-2(105)	W	39	5.92	49.5	850	2.7
148-6-4(105)	C	51	6.28	49.7	830	2.0
	C		6.33	51.4	—	1.7
	W		5.92	48.0	860	1.4
148-7-3(105)	C	59	5.79	44.5	962	3.7
	W		5.40	44.8	1150	2.5
148-8-3(15)	C	67	5.57	47.8	1002	3.7
	W		5.13	41.9	1214	4.8
148-9-4(105)	C	79	5.36	45.5	1391	5.1
	W		5.03	42.1	1600	4.4
148-10-3(105)	C	86	4.72	46.7	1662	4.4
	W		4.92	41.1	1420	4.7
148-12-4(105)	C	106	6.02	39.5	2200	2.8
	W		5.73	36.1	2370	3.6
148-14-3(105)	C	122	—	—	1990	4.2
	W		5.99	36.2	2370	5.2
148-16-3(105)	C	141	7.59	36.9	2320	2.6
148-18-2(105)	C	159	8.97	37.0	2250	1.3
	W		7.30	34.0	2414	1.8
148-20-3(105)	C	179	9.66	35.6	2180	1.6
	W		9.0	32.9	2450	1.9
148-23-4(95)	C	209	10.06	36.8	1730	0.7
	W		9.96	32.4	1990	1.9
148-26-2(15)	C	232	9.77	37.3	1312	0.7
	W		9.24	35.2	1520	0.7
	W		9.41	34.6	1345	1.0
149-2-2(105)	C	4	10.50	54.7	79	1.0
	W		10.08	51.9	95	1.0



TABLE 2 – Continued

Sample	Squeeze Type <sup>a</sup>	Depth (m)	Ca (m-g-at/l)	Mg (m-g-at/l)	NH <sub>4</sub> (μ-gr-at/l)	PO <sub>4</sub> (μ-gr-at/l)
149-2-5(105)	C	8	10.49	54.1	79	1.6
	W		10.45	53.0	68	1.4
149-3-5(105)	C	17	11.52	51.7	81	1.6
	W		11.52	51.8	83	1.1
149-4-3(105)	C	23	11.95	53.4	113	1.1
	W		11.85	52.6	103	1.4
149-5-3(120)	C	32	13.08	51.8	151	—
	W		12.73	49.8	120	1.1
149-6-4(105)	C	43	13.34	49.7	162	0.6
	W		—	—	150	—
149-7-2(105)	C	49	13.31	51.3	153	0.5
	W		13.06	49.7	139	0.8
149-8-4(105)	C	62	13.08	52.2	150	0.4
	W		13.66	49.1	141	0.5
149-9-5(105)	C	72	15.40	49.7	200	0.4
	W		14.90	47.7	156	0.5
149-10-2(120)	C	78	15.98	49.2	177	1.0
	W		15.85	46.5	165	0.8
149-11-4(120)	C	90	16.25	49.4	162	0.7
	W		15.90	46.0	216	0.7
149-12-5(120)	C	100	(17.10)	(37.4)	161	0.7
	W	Dye!!	(16.34)	(39.0)	139	—
149-14-3(120)	C	116	21.05	48.5	92	0.7
	W		20.18	41.9	138	1.1
149-16-4(15)	C	135	22.80	42.4	217	1.2
	W		22.52	40.4	248	1.0
149-18-3(120)	C	153	22.50	42.1	228	0.4
	W		22.25	41.3	236	0.7
149-20-4(120)	C	173	26.75	38.4	221	0.7
	W		26.00	38.4	156	1.0
149-23-4(120)	C	201	24.88	39.3	266	1.9
	W		23.64	38.1	236	2.4
149-26-2(120)	C	226	28.50	36.7	269	0.5
	W		28.60	34.3	280	0.5
149-29-3(120)	C	254	32.60	34.5	250	0.9
	W		29.80	33.5	176	0.6
149-31-1(120)	C	271	(28.34)	38.0	211	0.4
	W		(27.46)	35.6	220	0.9
149-33-1(120)	C	289	33.65	33.2	175	0.4
	W		31.10	33.3	235	0.2
149-35-4(120)	C	313	(30.60)	(34.6)	175	0.9
	W		31.40	35.0	283	0.9
149-37-3(120)	C	329	(29.7)	(36.0)	186	(8.1)
	W		31.10	34.0	122	0.5
149-40-1(100)	C	354	31.30	33.2	95	0.5
	W		28.85	33.8	109	—
149-41-5(120)	C	369	30.95	35.5	96	0.2
	W		31.10	36.9	137	0.5
149-42-2(120)	C	374	32.15	34.2	91	0.4
	W		30.60	35.2	114	0.2

<sup>a</sup>Squeeze types: C – cold, W – warm.

### Concentration gradients

Gradients in the concentrations of some of the major constituents of seawater have been reported by various authors both in the surface layers of sediments and also in the deeper holes of the Deep Sea Drilling Project (Presley and Kaplan, 1968; Sayles, Manheim and Chan, 1970; Sayles and Manheim, 1971). In sediments that show high rates of sedimentation, one often observes nonlinear gradients, or reversals in the gradients, e.g., Hole 30 of Leg 4 (Aves Ridge) and Holes 147 and 148, Leg 15. In sediments with accumulation rates between 2.5 and 1 cm/10<sup>3</sup>y, one generally observes that, if gradients do occur, they are

essentially linear in nature, e.g., Hole 63 of Leg 7, Holes 70, 71, and 72 of Leg 8, and Hole 149 of Leg 15.

Especially at fairly low rates of sedimentation, the existence of a concentration gradient implies transport through the interstitial water of the sediment, the gradients being functions of the rate of diffusion, the rate of sedimentation, and also of the rate of reaction in the processes for which gradients are observed. As is clear from Figures 6, 20 and 21, the calcium and magnesium gradients in Hole 149, which are respectively increasing and decreasing linearly to a depth of 240 meters, do not seem to depend on the nature of the sediment. Below 240 meters the calcium and magnesium remain essentially constant.

TABLE 3  
Saturation Calculations – Hole 149

Depth (m)	In situ P and T			1 atm and 4°C		
	Calculated	Observed	ΔpH	Calculated	Observed	ΔpH
3	8.0	7.65	0.35	7.8	7.8	0.0
18	7.85	7.40	0.45	7.7	7.6	0.1
50	7.80	7.55	0.25	7.7	7.6	0.1
78	7.80	7.3	0.5	7.7	7.5	0.2
117	7.6	7.3	0.3	7.6	7.5	0.1
136	7.7	7.2	0.5	7.5	7.4	0.1
173	7.3	7.0	0.3	7.25	7.3	-0.05
202	7.25	6.95	0.3	7.25	7.15	0.1
296	7.10	6.95	0.15	7.2	7.25	-0.05
360	7.15	6.95	0.15	7.3	7.3	0.0

Hole 29, which is situated about 30 km to the south of Hole 149 shows essentially the same sedimentary sequence as Hole 149, except that the first 270 meters of sediment in Hole 149 compare with only 130 meters in Hole 29. No large differences in the thickness are observed for the sequence of calcium carbonate rich radiolarian ooze in the lower parts of these holes. In Hole 29, no large gradients were observed in calcium and magnesium, despite the similarity in lithology between Hole 29 and Hole 149. From the constancy of the calcium and magnesium data below 250 meters in Hole 149, one can deduce that the main sink for magnesium is situated in these layers. Rex and Murray (1970) report the occurrence of sepiolite in the lower part of Hole 29. Whenever this authigenic magnesium silicate appears, the montmorillonite component is high and the calcium carbonate low. Also, dolomite is reported in these layers.

The fact that virtually no gradient is observed in magnesium in Hole 29, whereas in Hole 149 a steeply decreasing gradient with depth is found, may be explained from the fact that diffusional communication with the supernatant ocean water is more enhanced in Hole 29 than in Hole 149, the latter having nearly twice the sedimentation rate of Hole 29. This deserves further investigation.

In the lower part of Hole 149, dissolved silica values are about 1000  $\mu$ -gram-atoms/liter SiO<sub>2</sub> (Si), i.e., close to the saturation value of opaline silica. From the distribution of dissolved silica in Holes 147, 148, and 149 (Figures 4, 11, and 18), it is clear that no simple diffusional gradients exist for this component. The distribution and the values of dissolved silica seem directly related to the mineralogy at the depth of observation. Also, from the rapid change in the dissolved silica value upon a change in temperature, it appears that the dissolution kinetics are sufficiently rapid to nullify any gradients. This, of course, will make diffusional fluxes from sediments difficult to estimate. In Hole 149, no obvious gradients in silica are apparent in the surface layers of the sediment, nor in the bottom where the lowest sample was taken only 3 meters above a thick layer of chert (Figure 18).

#### Temperature Effects

As discussed before, the temperature effects of squeezing as determined during this cruise are of an approximate nature. The work of Mangelsdorf et al. (1969), Bischoff et

al. (1970), and Fanning and Pilson (1971) have indicated these temperature effects to exist, but little information is available on the reversibility and the kinetics of these effects. The results of this study only add information, but will not serve to explain the observed effects conclusively.

The effect of the temperature of squeezing was investigated only sporadically in Hole 147, and in detail in the Holes 148 and 149. The most interesting effect is on the dissolved reactive silica data (Figures 11 and 18). Similar effects were noticed by Fanning and Pilson (1971). The sediment sample has gone through a few cycles of temperature change, indicating that the effect is most likely reversible, but this evidence is not sufficient. Only if similar data are obtained after two or three temperature cycles do we have enough information on the reversibility. In Hole 148 the temperature effect seems to increase towards the bottom of the hole, but in Hole 149 the temperature effects display the same orders of magnitude, both in the low silica and in the high silica sediments. Of course, these experiments should be repeated under more carefully controlled conditions, because in the lower part of Hole 149, the temperature effects may have been suppressed due to insufficient temperature control on the warm squeeze.

The temperature of squeezing effect on dissolved inorganic phosphate is not clear (Figure 12), but is probably within the limits of error of the measurements. In Hole 148 (Figure 13), a distinct temperature effect is noticeable in the dissolved ammonia, but in Hole 149 (Figure 19), the scatter is too large to be conclusive. Of course, if ion exchange equilibria change with temperature, then there is no reason why NH<sub>4</sub><sup>+</sup> should not show such an effect. In general, univalent cations will tend to increase in concentration in the interstitial water with increasing temperature, whereas divalent cations will tend to show decreases. This is clearly mirrored in the distribution of calcium and magnesium.

The temperature effects are fairly uniform throughout the holes, except, perhaps, for calcium in Hole 149 (Figure 20). The effect for calcium is roughly  $0.5 \pm 0.3$  milli-gram-atoms/liter (slightly higher in the bottom of Hole 149) for a change of 19°C. For magnesium, the effect is  $3.0 \pm 0.5$  milli-gram-atoms/liter. These results are in qualitative agreement with the data of Bischoff et al. (1970). None of the observed gradients are severely affected by this temperature effect; at most, the slopes of the gradients would have to be adjusted slightly.

Finally, the effect of the temperature of squeezing on the alkalinity is not clear in Hole 148 (Figure 10), although below 100 meters the cold squeeze value seems systematically lower than the warm squeeze value. In Hole 149 (Figure 17), however, the effects are systematic, with a reversal occurring at a depth of 250 meters. The explanation of this effect is complicated by the fact that not only ion exchange but also calcium carbonate equilibria may have to be taken into account. In the upper part of Hole 149 for instance, the warm squeeze alkalinities are higher than those of the low temperature squeeze, but the dissolved calcium values show the reverse trend. It is conceivable that sufficient calcium is removed by ion exchange to cause undersaturation with respect to calcium carbonate, thus causing calcium carbonate dissolution with

a subsequent increase in alkalinity. In the deeper part of the hole, we may observe the opposite, i.e., removal of calcium ions by ion exchange may still leave the solution slightly supersaturated. Of course, anion exchange phenomena are not completely ruled out either.

#### Comparison With Other Techniques

Using preliminary data made available through the courtesy of the groups at Woods Hole Oceanographic Institute and at Texas A&M University (see elsewhere in this volume) a comparison could be made of the data for calcium and magnesium obtained by atomic absorption (AA) spectroscopy (Figures 23 and 24) and our complexometric data. From Figure 23, it appears that in the high alkalinity samples of Hole 147, calcium has been lost upon storage, presumably due to calcium carbonate precipitation. For all other samples, there seems to have occurred no such loss, and it appears that there is a slight systematic difference of less than 4 percent, the AA data being slightly higher. This difference is most likely due to a salt effect on our titer of the EGTA solution, which was standardized with pure  $\text{CaCO}_3$  dissolved in dilute hydrochloric acid. No salt effect was observed upon sodium chloride addition, but interference by sulfate ions could be a likely culprit. The apparent good agreement with the standard seawater provided by Woods Hole may, therefore, be fortuitous.

The systematic difference in the dissolved calcium data should show up as the dotted line in Figure 24 for magnesium, because my Mg data were obtained by subtracting the Ca + Sr from the Ca + Sr + Mg data. The scatter does not allow for a reasonable judgment. Table 4A gives a comparison of the standard seawater data of Woods Hole and my data. The data of Woods Hole agrees very well with the new Mg/Cl ratio of Carpenter (0.06626), whereas my data agrees with the old ratio of Culkin (0.0668) (Table 4). This could explain part of my higher magnesium data, but not the apparent discrepancy in the calcium data. In general, however, the data agree well and it can be concluded that, except for cases where the alkalinity is high (more than 20 milliequivalents/liter), calcium data are meaningful even when obtained from stored unacidified samples.

The alkalinity data compare less favorably (Figure 25). The data obtained by the Woods Hole group seem about 17 percent lower than my data, and show a large scatter. The shipboard data are estimated to be precise to better than 1 percent. The low alkalinities in Hole 147 for the Woods Hole data confirm the contention of calcium loss by precipitation.

#### REFERENCES

- Bader, R. G., 1955. Carbon and nitrogen relations in surface and subsurface marine sediments. *Geochim. Cosmochim. Acta*, 7, 205.  
 Berner, R. A., Scott, M. R. and Thomlinson, C., 1970. Carbonate alkalinity in the pore waters of anoxic marine sediments. *Limnol. and Oceanogr.* 15, 544.  
 Bischoff, J. L., Greer, R. E. and Luistro, A. O., 1970. Composition of interstitial waters of marine sediments: temperature of squeezing effect. *Science*, 167, 1245.

TABLE 4  
A. Seawater Mg-Content Comparisons

Woods Hole Data (m-g-at/l)	Gieskes Data (m-g-at/l)
53.9	55.0
54.5	54.9
53.8	54.4
53.4	55.0
	54.6
	54.9
Avg. 53.9	54.8(±0.5%)

B. Calculated Seawater Mg-Contents

Chlorinity (‰)	Mg <sup>a</sup>	Mg <sup>b</sup>
19.2	53.6	54.2
19.3	53.9	54.4
19.4	54.1	54.6

<sup>a</sup>Using Carpenter's Mg/Cl ratio (0.06626).

<sup>b</sup>Using Culkin's Mg/Cl ratio (0.0668).

- Drever, J. I., 1971. Magnesium-iron replacement in clay minerals in anoxic marine sediments. *Science*, 172, 1334.  
 Dyrssen, D., 1965. A Gran titration of seawater on board SAGITTA. *Acta Chem. Scand.* 19, 1265.  
 Edgar, N. T. and Saunders, J. B., 1971. Deep-Sea Drilling Project, Leg 15, *Geotimes*, 16, April 1971, 12.  
 Edmond, J. M., 1970. High precision determination of titration alkalinity and total carbon dioxide content of sea water by potentiometric titration. *Deep Sea Research* 17, 737.  
 Edmond, J. M. and Gieskes, J. M. T. M. 1970. On the calculation of the degree of saturation of sea water with respect to calcium carbonate under in situ conditions. *Geochim. Cosmochim. Acta*, 34, 1261.  
 Fanning, K. A. and Pilson, M. E. Q., 1971. Interstitial silica and pH in marine sediments: some effects of sampling procedures. *Science*, 173, 1228.  
 Garrels, R. M. and Thompson, M. E., 1962. A chemical model for seawater at 25°C and one atmosphere total pressure. *Am. J. Sci.* 60, 57.  
 Gran, G., 1952. Determination of the equivalence point in potentiometric titrations. Part 2. *Analyst*, 77, 861.  
 Heezen, B. C., Menzies, R. J., Broecker, W. S. and Ewing, W. M., 1958. Stagnation of the Cariaco Trench. Abstract, International Oceanographic Congress, New York, 1958.  
 Mangelsdorf, P. C., Jr., Wilson, T. R. S. and Daniell, E., 1969. Potassium enrichments in interstitial waters of recent marine sediments. *Science*, 165, 171.  
 Presley, B. J. and Kaplan, I. R., 1968. Changes in dissolved sulphate, calcium and carbonate from interstitial water of nearshore sediments. *Geochim. Cosmochim. Acta*, 32, 1037.  
 Presley, B. J., 1971. Techniques for analyzing interstitial water samples. Part 1: determination of selected minor and major inorganic constituents. In Winterer, E. L. et al., 1971. Initial Reports of the Deep Sea Drilling Project, Volume 7. Washington (U. S. Government Printing Office), 1749.  
 Rex, R. W. and Murray, B., 1970. X-ray mineralogy studies, Leg 4. In Bader, R. G. et al., 1970. Initial Reports of the

- Deep Sea Drilling Project, Volume 4. Washington (U. S. Government Printing Office), 325.
- Richards, F. A., 1965. Anoxic Basins and Fjords. *In* Chemical Oceanography, Volume I. (Eds. J. P. Riley and G. Shirrow). Academic Press. 611.
- Richards, F. A. and Vacarro, R. F., 1956. The Cariaco Trench, an anaerobic basin in the Caribbean Sea. *Deep Sea Research*. 3, 214.
- Sayles, F. L. and Manheim, F. T., 1971. Interstitial water studies on small core samples, Deep Sea Drilling Project, Leg 7. *In* Winterer, E. L., Reidel, W. R., et al., 1971: Initial Reports of the Deep Sea Drilling Project, Volume 7. Washington (U. S. Government Printing Office). 871.
- Sayles, F. L., Manheim, F. T., and Chan, K. M., 1970. Interstitial water studies on small core samples, Deep Sea Drilling Project, Leg 4. *In* Bader, R. G., Gerard, R. D., et al., 1970. Initial Reports of the Deep Sea Drilling Project, Volume 4. Washington (U. S. Government Printing Office). 401.
- Sholkovitz, E. R., 1971. Doctoral Thesis, University of California.
- Solorazano, L., 1969. Determination of ammonia in natural waters by the phenolhypochlorite method. *Limnol. Oceanogr.* 14, 799.
- Strickland, J. D. H. and Parsons, T. R., 1968. A practical handbook of sea water analysis. Fish. Res. Bd. of Canada, Bull. 167.
- Tsunogai, S., Nishimura, M., and Nakaya, S., 1968. Complexometric titration of calcium in the presence of larger amounts of magnesium. *Talanta*. 15, 385.